non-coding RNA

MDPI

Article

RNA N^6-methyladenosine affects copper-induced oxidative stress response in *Arabidopsis thaliana*

Bishwas Sharma[1,*], Ganesan Govindan[2,*], Yongfang Li[2], Ramanjulu Sunkar[2,*], and Brian D. Gregory[1,*]

[1] Department of Biology, University of Pennsylvania, Philadelphia PA 19104
[2] Department of Biochemistry and Molecular Biology, Oklahoma State University, Stillwater, OK 74078 USA
* Correspondence: ramanjulu.sunkar@okstate.edu and bdgregor@sas.upenn.edu

Abstract: Recently, post-transcriptional regulation of mRNA mediated by N^6-methyladenosine (m^{6}A) has been found to have profound effects on transcriptome regulation during plant responses to various abiotic stresses. However, whether this RNA modification can affect an oxidative stress response in plants has not been studied. To assess the role of m^{6}A modifications during copper-induced oxidative stress responses, m^{6}A-IP-seq was performed in Arabidopsis seedlings exposed to high levels of copper sulfate. This analysis revealed large-scale shifts in this modification on the transcripts most relevant for oxidative stress. This altered epitranscriptomic mark is known to influence transcript abundance and translation, therefore we scrutinized these possibilities. We found an increased abundance for the copper-enriched m^{6}A-containing transcripts. Similarly, we also found increased ribosome occupancy of copper-enriched m^{6}A-containing transcripts specifically those encoding proteins involved with stress responses relevant to oxidative stressors. Furthermore, the significance of the m^{6}A epitranscriptome on plant oxidative stress tolerance was uncovered by assessing germination and seedling development of the *mt*tant exposed to high copper treatment. These analyses suggested hypersensitivity of the *mta* mutant compared to the wildtype plants. Overall, our findings suggest an important role for the m^{6}A in oxidative stress response of Arabidopsis.

Keyw: N^6-methyladenosine; RNA modification; oxidative stress; Arabidopsis thaliana; plant stress response

1. Introduction

All living organisms rely on their ability to respond to the environmental changes ar[illegible]d them for their growth and survival. In general, plant species are sessile in nature, and therefore are constantly subjected to unfavorable abiotic and biotic environmental conditions. As a result, plants have evolved a variety of complex cellular response pathways that help them respond to both abiotic and biotic stresses, ultimately restoring and maintaining cellular homeostasis. These important response pathways are usually activated by biochemical molecules generated in the cells. Reactive oxygen species (ROS) are one such key species of biomolecules that are naturally formed as a byproduct of metabolism and, if left unchecked, can cause cellular and DNA damage. Therefore, the levels of ROS generated due to routine metabolic processes are usually regulated by ROS scavenging proteins that sequester them and prevent them from building up in the cells protecting them from damage. However, almost all stressors including drought[1], pathogens[2], unfavorable temperature[3], salinity, and heavy metals[4] in the soil can induce higher than usual amount of ROS spec[illegible]n plants and induce cellular damage inhibiting growth and development – a condition known as oxidative stress. During oxidative stress, many ROS species also simultaneously work as signaling molecules to help plants respond to this stress by inducing signaling pathways that activate genes key to its survival[5]

Citation: Sharma, B.; Govindan, G.; Li, Y.; Sunkar, R.; Gregory, B.D. RNA N^6-methyladenosine affects copper-induced oxidative stress response in *Arabidopsis thaliana*. *Non-Coding RNA* **2023**, *9*, x. https://doi.org/10.3390/xxxxx

Academic Editor(s):

Received: date
Revised: date
Accepted: date
Published: date

Copyright: © 2023 by the authors. Submitted for possible open access publication under the terms and conditions of the Creative Commons Attribution (CC BY) license (https://creativecommons.org/licenses/by/4.0/).

More recently, ROS molecules have been shown to affect epigenetic pathway of gene regulation in Arabidopsis, rice, and other plant species [1,6]. In Arabidopsis, histone deacetylases HDA19 and HDA9 were found to be inactivated as a result of oxidative stress, potentially leading to increased histone acetylation and alter associated gene expression[7]. Additionally, in pokeweed (*Phylotolacca americana L.*), the frequency of DNA methylation was shown to be partly mediated by ROS[8]. These studies suggest that ROS mediated stress response affects gene expression at different levels. Since ROS ~~species~~ are relatively short lived, the ROS response pathways are likely to also be regulated at post-transcriptional level for the plants to regulate their response quickly and precisely. While studies have investigated signal transduction of genetic and epigenetic pathways involving ROS, no study has yet investigated the possible epitranscriptomic regulation of oxidative stress response.

In the last decade, the diversity, and functions of epitranscriptomic modification of RNA have been studied in many organisms including more recently in plant species such as Arabidopsis, rice, and maize [9–11]. To date, hundreds of RNA modifications have been characterized [12] but functional studies of RNA modifications have been limited to a few modifications due to lack of molecular technology. Of these modifications, N6-methyladenosine or m^{6}A is the most prevalent mRNA modification found in most eukaryotic species. Functional studies have shown m^{6}A to be associated with mRNA stability [13,14], localization [15], splicing[16] and translation[17–19]. Recent studies have identified the role of m^{6}A in stress response. In plants, the loss of function mutant of m^{6}A writer protein MTA results in developmental delay as well as response to salt stress and cold stress [13,19,20]. Similarly, another study showed that ectopic expression of human m^{6}A demethylase FTO in rice and potatoes make them more tolerant to drought[21]. Since oxidative stress response pathway is intricately linked with many important abiotic and biotic stresses plants endure, it is highly likely that m^{6}A is also implicated in this pathway. To date, no studies have investigated the role of epitranscriptomic marks specifically under oxidative stress. Furthermore, in addition to mRNA, many studies have shown that non-coding RNAs are m^{6}A methylated [22,23] but to date no plant study has highlighted the possible regulation of non-coding RNA upon stress.

In this study, we investigate the change in the transcriptome-wide m^{6}A methylation profile during Arabidopsis oxidative stress response. There are several ways to induce oxidative stress in plants. For instance, studies have shown that exposure to high levels of copper ions (Cu^{2+}) induces excess levels of ROS accumulation in plants [5,24–26], and that this can provide a controllable system to induce oxidative stress in Arabidopsis. Using excess Cu^{2+} treatment, we performed m^{6}A RNA immunoprecipitation sequencing (me-RIP-seq) to investigate changes in m^{6}A status of transcripts. Additionally, we also look at changes in polysome binding of the transcripts whose m^{6}A enrichment status were most responsive to copper-induced oxidative stress. Furthermore, we have examined the impact of m^{6}A enrichment on long non-coding RNAs identified in our study.

2. Results

2.1. Reduction in global m^{6}A levels due to loss of MTA leads to lack of response to copper induced oxidative stress

To determine the effect(s) of the epitranscriptomic mark m^{6}A on plant oxidative stress response, we first investigated whether global reduction of methylation in the Arabidopsis transcriptome would have any effect on the ability of plants to respond to this stress. To do so, we used the previously well characterized post-embryonic loss of function mutant of the Arabidopsis m^{6}A writer protein MTA (*mta ABI3:MTA*; referred to hereafter as *mta*) [9]. Since complete loss of MTA is embryonic lethal, several studies have used this mutant that expresses the MTA writer protein only in the embryonic stages of development by using the embryo specific ABI3 promoter. Thus, we compared the survival and growth of these *mta* mutant as compared to wild-type Col-0 seedlings grown on control

MS agar plates and MS plates supplemented with copper sulfate at increasing concentrations of 100 and 125 µM. We found that both Col-0 and *mta* displayed overall decreased seedling growth and survival in the presence of increasing concentrations of copper. However, it was obvious that the *mta* mutant seedlings demonstrated a significant hypersensitivity to high levels of copper as compared to Col-0. Relatedly, we also observed that when grown vertically in the presence of increasing copper sulfate concentrations, the *mta* mutant displayed severely stunted primary root growth and seedling development compared to Col-0 plants (**Figure 1a**). Taken together, this data suggests that m^{6}A methylation of Arabidopsis transcripts is critical to the plant's ability to properly respond to oxidative stress induced by copper toxicity, particularly as the levels of this stress-inducing metal increases.

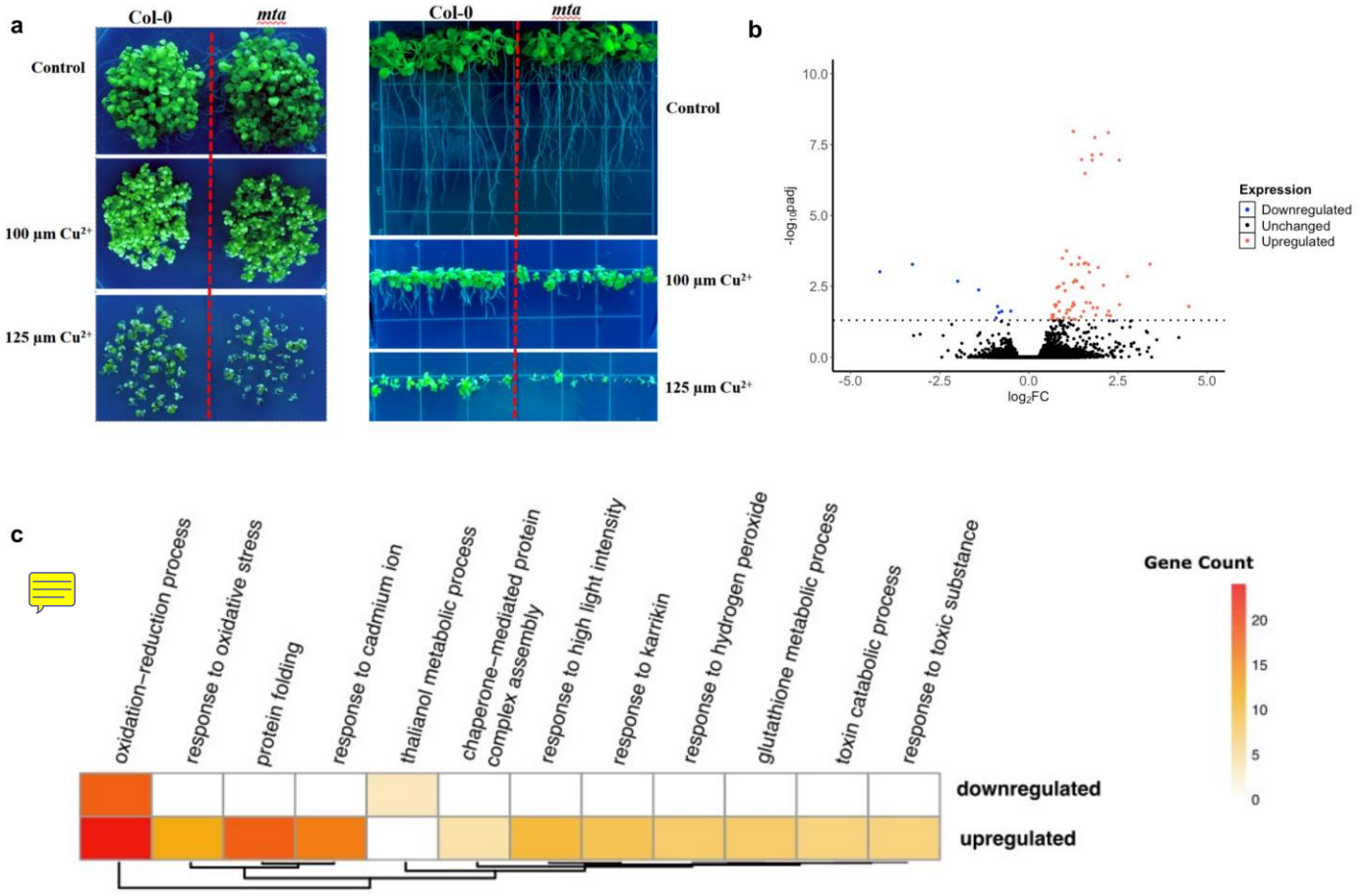


Figure 1. m^{6}A is involved in plant copper-induced oxidative stress response. a) Comparison of growth phenotypes between Col-0 and *mta* mutant seedlings under copper stress showing overall germination and survival when grown horizontally (left) and vertically (right) in a ½ strength MS agar supplemented with 100 µM Cu^{2+} and 125 µM Cu^{2+} in the media. Overall survival, root and shoot growth are all more severely affected in the *mta* mutant compared to Col-0 with increased strength of the stress. b) Volcano plot showing the transcriptome-wide change in transcripts upon copper stress for 24 hrs. The red and the pink dots represent transcripts that are meet our threshold of significantly decreased and increased (p-value < 0.05). c) Heatmap showing the number of genes significantly associated with various functional terms upon copper stress via GO analysis.

2.2. Copper induced stress increases the abundance of transcripts encoding proteins involved in responses to oxidative stress and pathogen defense

To understand the overall effect of oxidative stress on the Arabidopsis transcriptome, we subjected 20-day-old seedlings to oxidative stress by spraying with Cu^{2+} solution (see Methods for description) and measured the change in RNA abundance of the transcripts

after 24 hours using high throughput polyA⁺ selected RNA sequencing (RNA-seq). Differential expression (DE) analysis identified a total of 79 transcripts that displayed a statistically significant (adjusted p-value < 0.05) change in their overall abundance between stressed and unstressed conditions, with most of the messenger RNAs (mRNAs) displaying an increase in abundance (**Figure 1b**). Overall, although the transcriptome-wide RNA change was modest, Gene Ontology (GO) analysis revealed that transcripts associated with highly relevant biological processes were significantly altered in their abundance levels (**Figure 1c)**. Among these were transcripts encoding proteins that were previously shown to play significant roles in mediating oxidative stress, such as members of the glutathione transferase family (*GSTU2*, *GSTU4*, *GSTU9*, *GSTU19*, and *GSTU24*) as well as cysteine-rich receptor-like kinase 11 (*CRK11*) [27,28]. Additionally, as has previously been shown, copper treatment also induces defense response in the treated plants evident by an abundance increase in transcripts associated with the GO term "defense response to bacterium" (**Figure 1c)**.

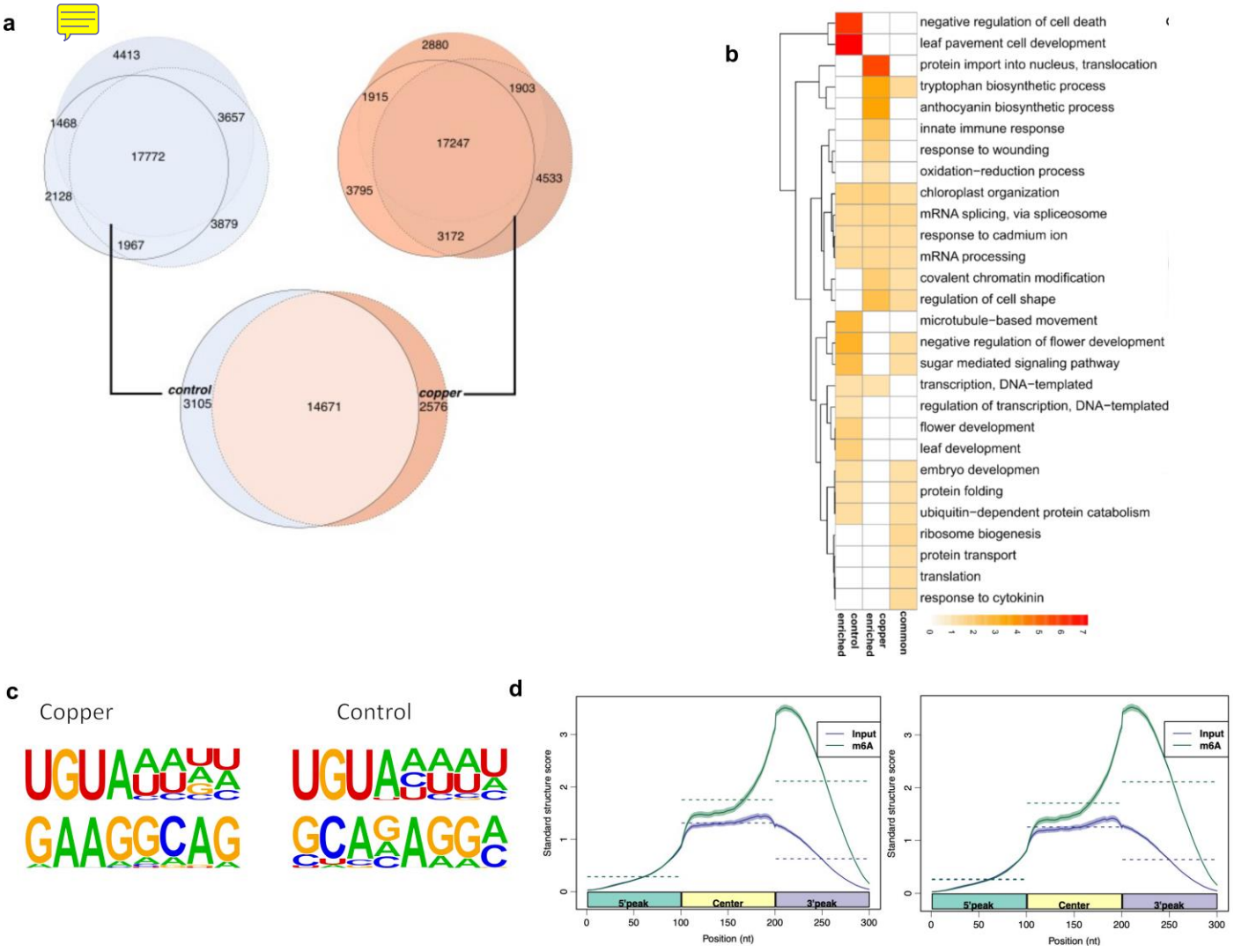


Figure 2. mRNA m⁶A dynamics in response to copper-induced oxidative stress. a) Venn diagrams showing overlap between the m⁶A peaks identified in the biological replicates within control (top left) and copper (top right) treatments. The overlapping peaks (or high confidence peaks) are then used to compare the m⁶A peaks detected between control and copper conditions (bottom). b) Two of the most significantly enriched motifs found in the m⁶A peak regions containing a canonical A site in both the copper and control conditions. c) Gene ontology for transcripts containing control-enriched, copper-enriched, or common m⁶A peaks between treatments.

2.3. Thousands of m⁶A peaks are specifically induced or depleted upon copper induced oxidative stress in mRNA

Next, we profiled the dynamic changes of m⁶A methylation in the overall Arabidopsis transcriptome upon oxidative stress treatment. To do this we carried out m⁶A-IP-seq, in which RNA fragments containing m⁶A are isolated via an m⁶A-specific antibody (SYSY:202008), and these purified sequences are subjected to high-throughput RNA sequencing as previously described [29]. Using the peak calling algorithm MACS2, we identified m⁶A peak regions in RNAs both in the presence and absence of copper stress. In total 17,772 and 17,247 high confidence m⁶A peaks were shared between the three biological replicates of copper and control treated samples, respectively (**Figure 2a**). By comparing these peaks between the stress and control groups, we found a notable difference in the m⁶A profile of the transcriptome with and without copper stress. Altogether, we identified 2,578 m⁶A peaks that were identified only under copper stress conditions and 3,105 that were found only under control conditions. These dynamic m⁶A peaks corresponded to 2,316 and 2,579 transcripts, respectively, which were subsequently referred to as stress-enriched and control-enriched m⁶A containing transcripts. Furthermore. the group containing the 14,671 transcripts with m⁶A peaks in both control and copper stress conditions (i.e., do not change their m⁶A levels upon stress) were referred to as "common" or "shared" transcripts between the two conditions. We performed GO analysis to investigate what functions the proteins encoded by these three groups of m⁶A methylated transcripts may play and found that many of the transcripts that contain the stress-enriched m⁶A peaks are associated with reaction to oxidation-reduction process, defense response, protein import, and anthocyanin production (**Figure 2b**). Conversely, the group of transcripts containing control-enriched m⁶A peaks were related to negative regulation of cell death, flowering, and other developmental processes. These results suggest that transcripts that help plants respond to oxidative stress were gaining m⁶A methylation specifically in response to stress treatment.

Since m⁶A-IP-seq does not provide nucleotide level resolution and gives a collection of mostly 150-200 base pair (bp) peak regions, we detected the enriched motifs in these m⁶A peak regions to provide a better idea of the actual methylated sites. Using the motif recognition algorithm HOMER, we found a previously annotated and potentially plant specific m⁶A motif UGUA as the top hit in these m⁶A peak regions from both control and copper stress m⁶A-IP-seq datasets [19,30], providing additional evidence of the high quality of our m⁶A-IP-seq datasets. Overall, the m⁶A-IP-seq data revealed m⁶A patterns that are characteristic of Arabidopsis as well as other plant and animals m⁶A studies with notable differences in the methylation profile under copper-induced oxidative stress as compared to control conditions (**Figure 2c**).

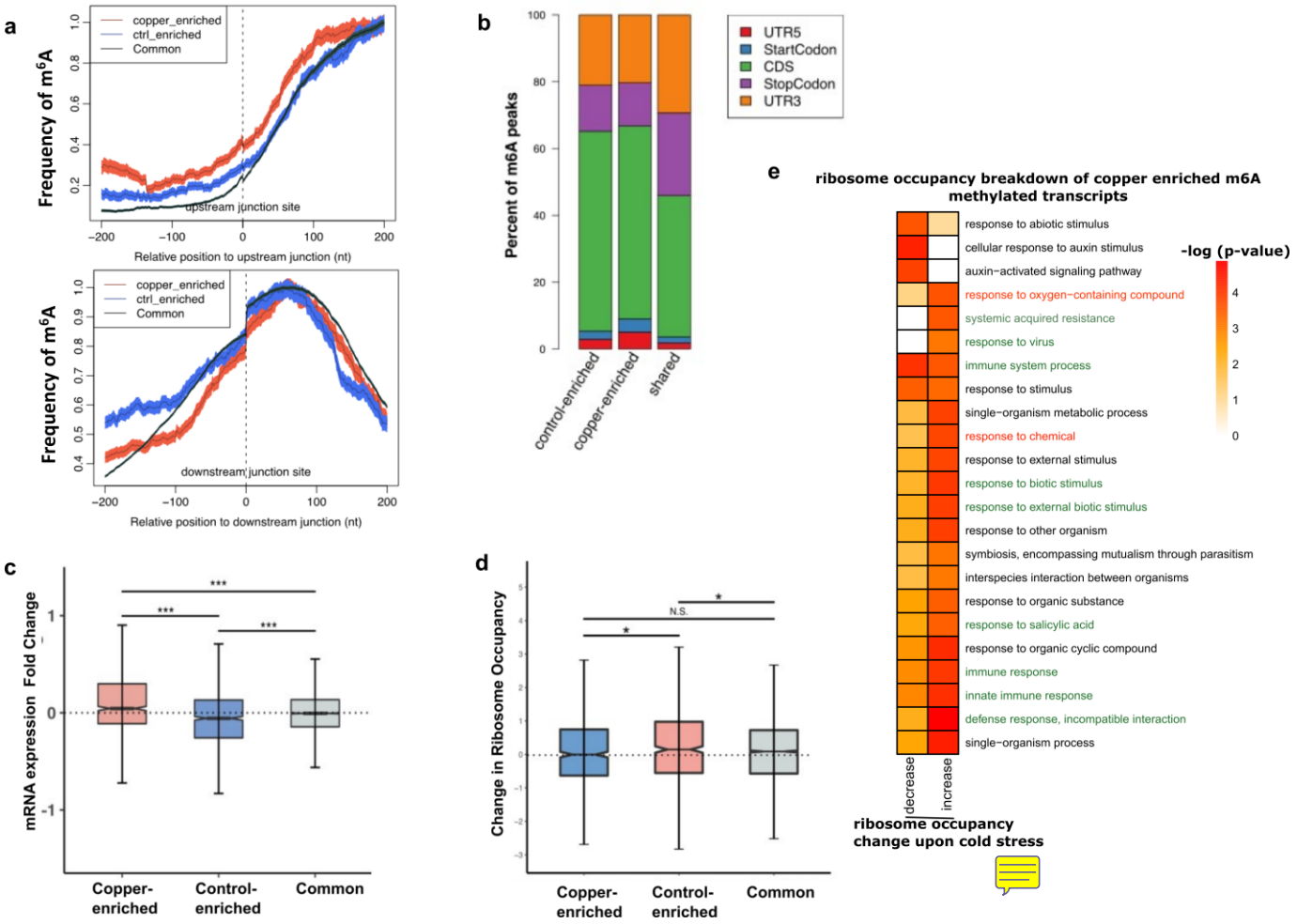


Figure 3. Copper-induced oxidative stress-specific m⁶A sites affect the abundance and translation of transcripts encoding proteins relevant to proper stress response. a) Percent breakdown of m⁶A peak regions in each category based on the region of transcript they overlap b) Per-nucleotide position frequency of methylation in the 200 nt region around the start codon (left) and stop codon (right). c) Change in RNA abundance measured as $\log_2$ fold change between copper stress and control for transcripts that contain either copper-enriched m⁶A, control-enriched m⁶A, or common m⁶A peaks are plotted in a box and whisker plot. All differences are significant (p-value < 0.001) based on Wilcoxon rank sum tests. d) Box and whisker plot of change in ribosome occupancy between control and copper stress conditions in the three categories of m⁶A methylated transcripts based on whether the methylation is enriched under stress only, enriched under control only, or found in both conditions. Significance was measured using Wilcoxon rank sum tests and found be significant (p-value < 0.01) for 2 of the three comparisons as indicated. e) Heatmap showing the functional terms enriched by GO analysis for transcripts that contain stress-enriched m⁶A based on whether they show positive or negative change (aka decrease or increase) in polysome association. The green highlighted terms are related to defense mechanisms and the red highlighted terms are related to oxidative stress response.

2.4. m⁶A tends to be localized in mRNA 3′ UTRs and its localization pattern is sensitive to copper-induced oxidative stress

To visualize the localization of m⁶A along the lengths of mRNA transcripts, we calculated the density of m⁶A-IP-seq reads in 100 nucleotide (nt) bins representing the 5′ UTR, coding region (CDS), and 3′ UTR regions of all detected mRNA transcripts. We observed that overall, both the control and copper treated samples displayed the same 3′ UTR bias in accumulation of reads in the m⁶A-IP-seq as compared to the background polyA⁺ RNA-seq datasets, which shows a strong enrichment of sequencing reads in the CDS region (**Figure 3d**). This 3′ UTR localization pattern of m⁶A is well established across

animal and plant species. Since we observed a large overlap between overall m^{6}A peaks between stress and control RNA, we next wanted to investigate whether there might be a change in m^{6}A localization pattern due to stress. To do this, we focused on the group of transcripts whose methylation status was sensitive to stress treatment. For this group of transcripts, we calculated the methylation frequency of each nucleotide position around the start and stop codon for the stress-enriched or control-enriched m^{6}A containing transcripts and plotted it against the many transcripts that do not change methylation status (labelled shared) upon stress treatment (**Figure 3a)**. Interestingly, we found that the frequency of methylation in the 5′ UTR was higher for transcripts containing stress-enriched m^{6}A compared to the other groups. Similarly, the percentage of unique m^{6}A peaks that overlapped with the 5′ UTR and start codons were also higher in transcripts that were either enriched or depleted in m^{6}A upon stress treatment compared to transcripts that showed no change in m^{6}A (**Figure 3b**). Overall, these results suggest that m^{6}A peaks that are sensitive to oxidative stress treatment have a higher probability of being deposited at the 5′ UTR or CDS regions, upstream of where m^{6}A is primarily found in the 3′ UTR. The mechanism by which this change in position dependent enrichment/depletion of m^{6}A warrants further studies.

2.5. Transcripts that contain copper stress enriched m^{6}A are more likely to show increased mRNA levels.

It has been previously suggested that m^{6}A can affect transcript stability and abundance. A recent study from our group showed that transcripts that are enriched for m^{6}A upon stress showed a positive trend in transcript expression level in the context of cold stress [19]. To test for any such correlations that exist in the context of oxidative stress, we used m^{6}A profiling data and the RNA-seq data. After determining the fold-change in expression for each transcript, we categorized the values based on whether the transcript contains m^{6}A that is affected by copper treatment and plotted them on a box and whisker plot (**Figure 3c)**. Overall, we saw that transcripts with copper stress induced m^{6}A peaks displayed significantly increased transcript abundance compared to those that contain copper stress-depleted m^{6}A or unchanged m^{6}A peaks. The group of transcripts that lost their m^{6}A methylation status upon copper treatment showed, on average, a more negative change in transcript abundance in the context of copper-induced oxidative stress response. Thus, gaining m^{6}A during this stress response tended to correlate with overall increased abundance for the transcripts gaining this methylation event.

2.6. Copper stress induced m^{6}A are more likely to be polysome associated.

While stress induced m^{6}A was associated with change in overall transcript abundance, the actual number of differentially expressed transcripts upon copper stress treatment in our study was still relatively low as discussed previously. We therefore investigated whether m^{6}A had other downstream effects on the transcript fate, specifically on translation. Although not a perfect measure of translation, we looked at polysome association as a proxy to study the effect of m^{6}A on the ratio of transcripts that were bound to polysomes. To do this, we generated polysomal sequencing libraries by pulling down polysome fractions and extracting the RNA bound to them. Using polysome occupancy as a measurement, we plotted the change in occupancy of transcripts under stress to measure effects on translation due to m^{6}A (**Figure 3d**). From this analysis, we observed a relatively higher and statistically significant polysome association of transcripts containing stress enriched m^{6}A compared to those containing control enriched or shared m^{6}A. To further investigate which transcripts are responsible for the higher average polysome association among those that were copper enriched, we broke down the category into those that show positive value for polysome occupancy change and those that show a negative value. Gene Ontology analysis shows that transcripts relevant to oxidative stress response terms such as “response to oxygen containing compounds” and defense related terms showed

increased polysome association in the context of copper treatment (**Figure 3e)**. Therefore, these transcripts are enriched for m⁶A upon stress and show increased binding to polysomes serving as candidates for investigating molecular mechanisms of m⁶A regulation of translation in the context of oxidative stress in the future.

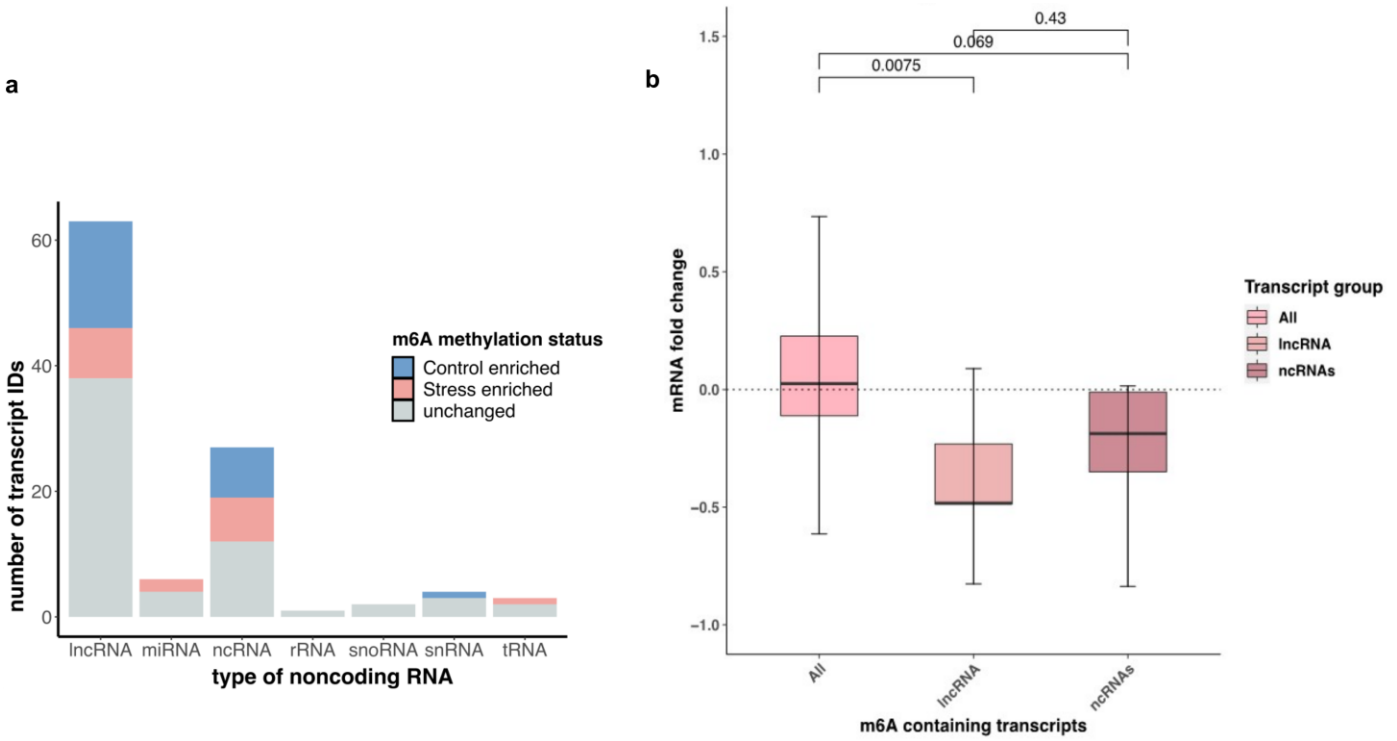


Figure 4. Long non-coding (lncRNA) m⁶A dynamics in response to copper-induced oxidative stress. a) Stacked bar graph showing the total number of unique non-coding RNAs of various known categories or labelled as ncRNA if category is not clear in the annotation. Breakdown of ncRNA based on number of transcripts containing stress-enriched m⁶A (red bar), control enriched m⁶A (blue bar), or m⁶A that is common or unchanged between conditions (grey bar). b) For ncRNA and lncRNA transcripts containing stress-induced m⁶A, box and whisker plot showing change in mRNA levels after copper stress treatment.

2.7. Long noncoding RNAs (lncRNAs) and m⁶A association

Various classes of non-coding RNAs (ncRNAs) have previously been shown to contain m⁶A in many plant studies that performed global profiling of m⁶A [22,23]. Although the most highly abundant ncRNAs – ribosomal RNAs (rRNAs) and transfer RNAs (tRNAs) are non-polyadenylated and therefore not captured by our m⁶A-IP-seq experiments, many other types of ncRNAs including long noncoding RNAs (lncRNAs) as well as precursors for microRNAs (miRNAs) and snoRNAs have been found to contain a polyA⁺ tail. A recent study conducted a global profiling of lncRNAs in Arabidopsis [31] using both polyA⁺ and polyA⁻ methods and found that a significantly higher number of lncRNAs (1,352) were polyadenylated as opposed to those that were not (198) suggesting that lncRNAs were almost 7 times more likely to be polyadenylated than not. Therefore, our polyA⁺ RNA-seq data can be used for studying m⁶A profiles in polyadenylated ncRNAs under oxidative stress. Using the annotations for different classes of ncRNAs loci from the ENSEMBL database, we compared the m⁶A peak information to detected m⁶A peaks found within the ncRNA regions. Among all methylated ncRNAs in our dataset, lncRNAs had the highest number of transcripts followed by general ncRNAs that were not categorized into the other types (**Figure 4a)**. Furthermore, these methylated transcripts, when separated by the effect of oxidative stress on the m⁶A methylation, show that there are various lncRNAs and ncRNAs that are enriched for m⁶A upon copper

treatment. Next, we inquired whether the ncRNA transcripts containing stress-induced m^{6}A showed a similar pattern of positive RNA abundance change upon stress as protein-coding mRNAs of this category. Surprisingly, these ncRNA transcripts instead showed an overall negative transcript abundance upon stress contrary to the overall trend of stress induced m^{6}A-containing mRNA transcripts (**Figure 4b)**. This contradictory pattern suggests that m^{6}A mediated RNA response might be different between coding and non-coding RNA, particularly mRNAs as compared to lncRNAs. Further exploring this observation is an interesting question for future research.

3. Discussion

Oxidative stress is a complex physiological phenomenon that occurs simultaneously with, or a result of, almost every abiotic and biotic stress condition faced by plants. It is crucial for plants to respond to oxidative stress to protect their cellular components from damage that can result from accumulation of ROS. As such it is highly likely that the regulation of gene expression in the oxidative stress response pathway happens at genetic, epigenetic, and possibly epitranscriptomic levels. While we have evidence of such regulation in the genetic and epigenetic levels, the role of epitranscriptomic RNA regulation in ROS response is largely unknown. Our study suggests that epitranscriptomic RNA modification m^{6}A is involved in oxidative stress response.

Exposure of Arabidopsis seedlings to copper ions induces oxidative stress, triggering molecular response pathways that help them cope with the physiological changes brought about by heavy metal. Although our treatment did not trigger a massive shift in the RNA expression profile, the genes that showed statistically significant differential expression of RNA abundance upon oxidative stress were mostly genes responsive to oxidative stress response, such as those belonging to the glutathione transferase family as well as other relevant functions.

In contrast to the modest number of genes showing a statistically significant RNA level change, we saw many transcripts that contained m^{6}A which was either enriched or depleted upon oxidative stress. Overall, a significantly more positive change in transcript abundance was seen in transcripts with stress enriched m^{6}A while a negative change was seen in those with depleted m^{6}A. This suggests that dynamic methylation is positively associated with transcript abundance. On the other hand, transcripts that showed no change in m^{6}A between stress and control on average showed no such change in transcript abundance. This raises the question whether there is anything different about this stress sensitive methylation. The m^{6}A peak distribution across mRNA features as well as the normalized m^{6}A frequency plot shows that a small fraction of these stress enriched or depleted m^{6}A peaks are slightly more likely to be found on the 5′ UTR, start codon, and CDS regions than the peaks whose presence does not change upon stress. However, a mechanism that explains why these "upstream" peaks could affect transcript stability differently are yet to be understood.

On the other hand, it has been shown in mammalian systems that a 5′ UTR m^{6}A can affect translation via an m^{6}A reader protein where it can increase the rate of translation of methylated transcripts via a cap independent translation mechanism [18]. We were curious to see if there was any effect on translation status of methylated transcripts specifically under stress conditions. Our results show that overall polysome occupancy, which we are considering proxy metric for translation status, is changing more positively for the transcripts containing stress enriched m^{6}A. Breakdown of this group of transcript shows that oxidative stress response and defense response genes are driving the average polysome occupancy change to be more positive. Thus, the average of both metrics of gene expression (transcript abundance and polysome association upon oxidative stress) displayed a positive increase for those copper stress enriched m^{6}A containing transcripts. It is, however, important to note that a considerable number of the transcripts in these m^{6}A categories show the opposite/negative trend in transcript abundance and polysome association. Therefore, there is likely an unknown mechanism that provides a much-needed functional

specificity to m^{6}A's role, one that most likely includes m^{6}A reader-dependent mechanism – reading of these changes by a specific m^{6}A reader protein.

Non-coding RNAs are essential for gene regulation. In our analysis we found various classes of ncRNAs were methylated both before and during copper-induced oxidative stress response. Among them, lncRNAs had the highest number of transcripts that contained stress induced and stress depleted m^{6}A. We were curious whether we would see a positive change in transcript abundance in the lncRNA transcripts with the stress enriched m^{6}As. On the contrary, we saw a negative change in transcript abundance for the lncRNAs which suggests that the m^{6}A dependent regulation of lncRNA may differ from that ncRNA compared to mRNA. This interesting finding will be explored in future research.

4. Materials and Methods

Stress treatment for RNA-seq, m^{6}A-IP-seq, and polysomal RNA-seq

Surface sterilized *Arabidopsis thaliana* seeds from Col-0 accession were plated on ½ Murashige and Skoog (MS) solid medium, vern[illegible] for 48hr under dark, then were transferred to a 22°C growth chamber where the plants were grown under a 12/12 hour light and dark cycle for three weeks. For copper treatment seedlings were then sprayed with 100 μM $CuSO_4$ while seedlings without treatment served as controls. After 24 hours of treatment, whole seedlings from both control and copper-treated seedlings were harvested and stored at -80°C until RNA extraction.

m^{6}A RNA immunoprecipitation and sequencing (m^{6}A-IP-seq)

The immunoprecipitation of m^{6}A containing RNA fragments was done as described previously [19]. Briefly, total RNA was extracted from the copper treated and control samples using TRIzol and the quality of RNA was checked using 1.2% agarose gel. After using Nanodrop ND-1000 to measure the total RNA concentration, 120 μg of total RNA was used for poly(A) RNA purification using Arraystar Seq-StarTM poly(A) mRNA Isolation Kit separately for three biological replicates. Purified polyadenylated RNA was chemically fragmented using 10 mM Zn^{2+} at 94°C for 5 minutes in 10 mM Tris-HCl (pH 7.0) buffer. After analyzing the size of the fragments using an Agilent 2100 Bioanalyzer, an aliquot of the fragmented polyA$^+$ RNA was immunoprecipitated using 2 μg anti-m^{6}A rabbit polyclonal antibody (Synaptic Systems) in a 500 μl IP reaction in the IP buffer (10 mM Tris-HCl at pH7.4, 150 mM NaCl, 0.1% NP-40) at 4°C for two hours. 20 μL Dynabeads™ M-280 Sheep Anti-Rabbit IgG was prepared and incubated with the IP mixture for two hours at 4°C and washed 3X with IP buffer and 2X with wash buffer (10 mM Tris-HCl at pH7.4, 50 mM NaCl, 0.1% IGEPAL CA-630). The resulting immunoprecipitated m^{6}A containing RNA fragments were eluted in a 10 mM Tris-HCl at pH7.4 containing 1 mM EDTA, 0.05% SDS, and 40U proteinase K at 50°C for 30 minutes. The RNA fragments were purified using phenol-chloroform extraction protocol and precipitated with ethanol. The resulting m^{6}A containing mRNA fragments were used to construct m^{6}A-IP-seq library using KAPA stranded mRNA-seq Kit (Illumina® platform) and sequenced on the Illumina HiSeq 4000 platform. In parallel, aliquots of the fragmented polyA$^+$ RNA without the immunoprecipitation were used to generate three biological replicates of background polyA$^+$ RNA-seq library for both control and stress treated samples.

Polysomal RNA-sequencing

Under the same conditions as the m^{6}A-IP-seq, polysomes were isolated from three-week-old Arabidopsis seedlings grown under control or 24 hours of copper treatment as described previously [32]. For treated and untreated samples, two biological replicate tissues were ground into a fine powder using liquid nitrogen and used for polysome extraction. Approximately 500 mg of powdered tissue was thoroughly resuspended in 1250 μL polysome extraction buffer (200 mM Tris (pH 9.0), 200 mM KCl, 26 mM $MgCl_2$, 25mM EGTA, 100 μM 2-mercaptoethanol, 50 μg/ml cycloheximide, 50 μg/ml chloramphenicol,

1% Triton X-100, 1% Brij-35, 1% Tween-40, 1% IGEPAL CA-630, 2% polyoxyethylene-10-tridecyl ether, 1% deoxycholic acid) and incubated for 10 minutes on ice with occasional mixing. The polysome was separated using centrifugation at 14000 rpm for 2m[illegible] at 4°C. The resulting supernatant fraction was layered on sucrose density gradients (20–60% sucrose, w/v) and centrifuged for 120 min at 40,000 rpm (275,000 g) in a Beckman OPTIMA LE-80 centrifuge. Using UA-5 detector and a Gradient Fractionator (model 640, ISCO), optical densities of the gradient fractions were measured at 254 nm. For polysome RNA, sucrose fractions with more than two ribosomes were pooled and extracted using TRIzol reagent. Approximately 8 µg polysome associated RNA per replicate was subjected to polyA$^+$ selection followed by RNA-seq library preparation using KAPA Stranded mRNA-seq Kit (Illumina® platform). After validating the library quality using Agilent 2100 Bioanalyzer, the polysomal sequencing library was sequenced using Illumina HiSeq 4000 platform.

Bioinformatics analysis of RNA-seq, m^{6}A-IP-seq, and polysome-seq data

Read Processing

Sequencing files generated from HiSeq 4000 platform in raw fastq format were quality checked using the bioinformatic package FastQC [33]. Using Trimmomatic-0.36, the Illumina sequencing adapters were trimmed from raw reads using the tool Trimmomatic-0.36 and the provided Truseq3-SE adapter sequences [34]. Trimmed fastq sequences were mapped to Arabidopsis genome assembly TAIR10 downloaded from the ENSEMBL database using STAR aligner to generate BAM files using parameters: --outSAMattributes All and --outSAMtype BAM [35].

Differential RNA abundance

To calculate the RNA abundance, the count feature of python package HTSeq [36] was used to assign the number raw reads in the BAM files to gene IDs annotated in the TAIR10 reference annotation file obtained from ENSEMBL repository in a strand specific manner. These raw counts were then used as input for an R statistical package DESeq2 [37] using its default settings which uses normalization factors that incorporate library depth and gene wide dispersions for normalization of the reads and determines the change in expression in the form of fold change (log converted) between control and stress treatments and respective p-values of the difference. Transcripts that showed adjusted p-value of <0.05 were called significant.

m^{6}A peak calling

As described previously we used peak calling software MACS2 to call m^{6}A peaks [38]. Briefly, peaks were called using the alignment bam files of the m^{6}A-IP-seq and the background mRNA-seq as input with parameters as described previously [39]. Briefly, in order to preserve the strand information, the reads in the bam files were split using SAMtools [40] based on the strand they aligned to. Peaks were then called separately for the plus and minus strands for each condition and each replicate using parameters –no-model. The input polyA RNA that was used as background for STAR was also split based on plus and minus strand. Peaks were filtered by p-values < 0.05. The output was a NarrowPeak file that contained the loci of peaks identified by MACS2.

Motif searches

Sequence motifs enriched in the m^{6}A peak regions in the narrowpeak files were searched using the *de novo* motif search algorithm HOMER [41]. In simple words, HOMER looks for sequence features that are enriched in a list of provided sequences against randomized background of nucleotides reads with matched GC% content along with the possible false positive ratio. In this case, the sequences provided to HOMER were extracted

by comparing the peak loci in the narrowpeak files to the annotated reference transcript sequence.

m^{6}A frequency

For the transcripts grouped by whether m^{6}A it contained was enriched, depleted, or remain unchanged by copper induced oxidative stress, the frequency of m^{6}A methylation for each nucleotide position near the start or stop codon was calculated using the following formula:

$$\text{frequency} = (\text{number of unique m}^6\text{A peak regions that overlapped with that nucleotide position/ the total number of transcripts that were m}^6\text{A methylated})$$

The frequency value for each category of transcripts was then normalized to the maximum frequency value within the 200nt region flanking the start or stop codon to visualize the trend of m^{6}A in these boundary regions in each category of transcripts.

Polysome occupancy

The polysome occupancy of each transcript was determined by first normalizing the raw read count of each transcript within each replicate to the sequencing depth of the library and calculating the read per million (RPM) value. Polysome occupancy value for each transcript was then calculated as:

$$\text{polysome occupancy} = \log_2 (\text{RPM from polysome sequencing / RPM in the RNA-seq}).$$

In order to determine the effect of copper stress on polysome occupancy of RNA, we calculated the change in occupancy value for each transcript with and without stress using the formula:

$$\text{Polysome occupancy change} = \text{Polysome Occupancy}_{\text{copper}} - \text{Polysome Occupancy}_{\text{control}}$$

The difference is the log transformed polysome occupancy values where a negative value represents a decrease in polysome occupancy while a positive value means an increase in occupancy upon oxidative stress.

Author Contributions: Conceptualization, B.D.G. and R.S.; methodology, B.S., G.G., and Y.L.; software, B.S. and B.D.G.; validation, B.S., G.G., and Y.L.; formal analysis, B.S.; investigation, B.S., G.G., Y.L., R.S. and B.D.G.; resources, B.D.G.; data curation, B.S..; writing—original draft preparation, B.S. and B.D.G.; writing—review and editing, R.S.; visualization, B.S.; supervision, R.S. and B.D.G.; project administration, R.S. and B.D.G.; funding acquisition, R.S. and B.D.G. All authors have read and agreed to the published version of the manuscript.

Funding: "This research was funded by the United States National Science Foundation, grant numbers IOS-20233010 and IOS-1849708 to B.D.G. The funders had no role in study design, data collection and analysis, decision to publish, or preparation of the manuscript.

Data Availability Statement: The sequencing data presented in this manuscript can be found in GEO under the accession number: ######.

Acknowledgments: The authors thank all past and present members of the Gregory and Sunkar labs.

Conflicts of Interest: The authors declare no conflict of interest.

References

1. Lee, S.; Seo, P.J.; Lee, H.-J.; Park, C.-M. A NAC Transcription Factor NTL4 Promotes Reactive Oxygen Species Production during Drought-Induced Leaf Senescence in Arabidopsis. *Plant J* **2012**, *70*, 831–844, doi:10.1111/j.1365-313X.2012.04932.x.

2. Yang, C.; Li, W.; Cao, J.; Meng, F.; Yu, Y.; Huang, J.; Jiang, L.; Liu, M.; Zhang, Z.; Chen, X.; et al. Activation of Ethylene Signaling Pathways Enhances Disease Resistance by Regulating ROS and Phytoalexin Production in Rice. *Plant J* **2017**, *89*, 338–353, doi:10.1111/tpj.13388.
3. Kawarazaki, T.; Kimura, S.; Iizuka, A.; Hanamata, S.; Nibori, H.; Michikawa, M.; Imai, A.; Abe, M.; Kaya, H.; Kuchitsu, K. A Low Temperature-Inducible Protein AtSRC2 Enhances the ROS-Producing Activity of NADPH Oxidase AtRbohF. *Biochimica et Biophysica Acta (BBA) - Molecular Cell Research* **2013**, *1833*, 2775–2780, doi:10.1016/j.bbamcr.2013.06.024.
4. Sunkar, R.; Kapoor, A.; Zhu, J.-K. Posttranscriptional Induction of Two Cu/Zn Superoxide Dismutase Genes in Arabidopsis Is Mediated by Downregulation of MiR398 and Important for Oxidative Stress Tolerance. *Plant Cell* **2006**, *18*, 2051–2065, doi:10.1105/tpc.106.041673.
5. Jagadeeswaran, G.; Li, Y.-F.; Sunkar, R. Redox Signaling Mediates the Expression of a Sulfate-Deprivation-Inducible MicroRNA395 in Arabidopsis. *Plant J* **2014**, *77*, 85–96, doi:10.1111/tpj.12364.
6. Zhou, H.; Finkemeier, I.; Guan, W.; Tossounian, M.-A.; Wei, B.; Young, D.; Huang, J.; Messens, J.; Yang, X.; Zhu, J.; et al. Oxidative Stress-Triggered Interactions between the Succinyl- and Acetyl-Proteomes of Rice Leaves. *Plant Cell Environ* **2018**, *41*, 1139–1153, doi:10.1111/pce.13100.
7. Liu, P.; Zhang, H.; Yu, B.; Xiong, L.; Xia, Y. Proteomic Identification of Early Salicylate- and Flg22-Responsive Redox-Sensitive Proteins in Arabidopsis. *Sci Rep* **2015**, *5*, 8625, doi:10.1038/srep08625.
8. Jing, M.; Zhang, H.; Wei, M.; Tang, Y.; Xia, Y.; Chen, Y.; Shen, Z.; Chen, C. Reactive Oxygen Species Partly Mediate DNA Methylation in Responses to Different Heavy Metals in Pokeweed. *Front Plant Sci* **2022**, *13*, 845108, doi:10.3389/fpls.2022.845108.
9. Zhong, S.; Li, H.; Bodi, Z.; Button, J.; Vespa, L.; Herzog, M.; Fray, R.G. MTA Is an Arabidopsis Messenger RNA Adenosine Methylase and Interacts with a Homolog of a Sex-Specific Splicing Factor. *Plant Cell* **2008**, *20*, 1278–1288, doi:10.1105/tpc.108.058883.
10. Cheng, P.; Bao, S.; Li, C.; Tong, J.; Shen, L.; Yu, H. RNA N6-Methyladenosine Modification Promotes Auxin Biosynthesis Required for Male Meiosis in Rice. *Developmental Cell* **2022**, *57*, 246-259.e4, doi:10.1016/j.devcel.2021.12.014.
11. Yang, X.; Yang, Y.; Sun, B.-F.; Chen, Y.-S.; Xu, J.-W.; Lai, W.-Y.; Li, A.; Wang, X.; Bhattarai, D.P.; Xiao, W.; et al. 5-Methylcytosine Promotes MRNA Export - NSUN2 as the Methyltransferase and ALYREF as an M5C Reader. *Cell Res* **2017**, *27*, 606–625, doi:10.1038/cr.2017.55.
12. Boccaletto, P.; Stefaniak, F.; Ray, A.; Cappannini, A.; Mukherjee, S.; Purta, E.; Kurkowska, M.; Shirvanizadeh, N.; Destefanis, E.; Groza, P.; et al. MODOMICS: A Database of RNA Modification Pathways. 2021 Update. *Nucleic Acids Res* **2022**, *50*, D231–D235, doi:10.1093/nar/gkab1083.
13. Kramer, M.C.; Janssen, K.A.; Palos, K.; Nelson, A.D.L.; Vandivier, L.E.; Garcia, B.A.; Lyons, E.; Beilstein, M.A.; Gregory, B.D. N6-Methyladenosine and RNA Secondary Structure Affect Transcript Stability and Protein Abundance during Systemic Salt Stress in Arabidopsis. *Plant Direct* **2020**, *4*, e00239, doi:10.1002/pld3.239.
14. Du, H.; Zhao, Y.; He, J.; Zhang, Y.; Xi, H.; Liu, M.; Ma, J.; Wu, L. YTHDF2 Destabilizes m(6)A-Containing RNA through Direct Recruitment of the CCR4-NOT Deadenylase Complex. *Nat Commun* **2016**, *7*, 12626, doi:10.1038/ncomms12626.
15. Flamand, M.N.; Meyer, K.D. M6A and YTHDF Proteins Contribute to the Localization of Select Neuronal MRNAs. *Nucleic Acids Res* **2022**, *50*, 4464–4483, doi:10.1093/nar/gkac251.
16. Hou, Y.; Sun, J.; Wu, B.; Gao, Y.; Nie, H.; Nie, Z.; Quan, S.; Wang, Y.; Cao, X.; Li, S. CPSF30-L-Mediated Recognition of MRNA M6A Modification Controls Alternative Polyadenylation of Nitrate Signaling-Related Gene Transcripts in Arabidopsis. *Mol Plant* **2021**, *14*, 688–699, doi:10.1016/j.molp.2021.01.013.
17. Li, A.; Chen, Y.-S.; Ping, X.-L.; Yang, X.; Xiao, W.; Yang, Y.; Sun, H.-Y.; Zhu, Q.; Baidya, P.; Wang, X.; et al. Cytoplasmic M6A Reader YTHDF3 Promotes MRNA Translation. *Cell Res* **2017**, *27*, 444–447, doi:10.1038/cr.2017.10.
18. Meyer, K.D.; Patil, D.P.; Zhou, J.; Zinoviev, A.; Skabkin, M.A.; Elemento, O.; Pestova, T.V.; Qian, S.-B.; Jaffrey, S.R. 5′ UTR M6A Promotes Cap-Independent Translation. *Cell* **2015**, *163*, 999–1010, doi:10.1016/j.cell.2015.10.012.
19. Govindan, G.; Sharma, B.; Li, Y.; Armstrong, C.D.; Merum, P.; Rohila, J.S.; Gregory, B.D.; Sunkar, R. MRNA N6 -Methyladenosine Is Critical for Cold Tolerance in Arabidopsis. *Plant J* **2022**, doi:10.1111/tpj.15872.
20. Hu, J.; Cai, J.; Park, S.J.; Lee, K.; Li, Y.; Chen, Y.; Yun, J.-Y.; Xu, T.; Kang, H. N6 -Methyladenosine MRNA Methylation Is Important for Salt Stress Tolerance in Arabidopsis. *Plant J* **2021**, *106*, 1759–1775, doi:10.1111/tpj.15270.
21. Yu, Q.; Liu, S.; Yu, L.; Xiao, Y.; Zhang, S.; Wang, X.; Xu, Y.; Yu, H.; Li, Y.; Yang, J.; et al. RNA Demethylation Increases the Yield and Biomass of Rice and Potato Plants in Field Trials. *Nat Biotechnol* **2021**, *39*, 1581–1588, doi:10.1038/s41587-021-00982-9.
22. Bhat, S.S.; Bielewicz, D.; Gulanicz, T.; Bodi, Z.; Yu, X.; Anderson, S.J.; Szewc, L.; Bajczyk, M.; Dolata, J.; Grzelak, N.; et al. MRNA Adenosine Methylase (MTA) Deposits M6A on Pri-MiRNAs to Modulate MiRNA Biogenesis in Arabidopsis Thaliana. *Proc Natl Acad Sci U S A* **2020**, *117*, 21785–21795, doi:10.1073/pnas.2003733117.
23. Liu, N.; Parisien, M.; Dai, Q.; Zheng, G.; He, C.; Pan, T. Probing N6-Methyladenosine RNA Modification Status at Single Nucleotide Resolution in MRNA and Long Noncoding RNA. *RNA* **2013**, *19*, 1848–1856, doi:10.1261/rna.041178.113.
24. Sunkar, R.; Bartels, D.; Kirch, H.-H. Overexpression of a Stress-Inducible Aldehyde Dehydrogenase Gene from Arabidopsis Thaliana in Transgenic Plants Improves Stress Tolerance. *Plant J* **2003**, *35*, 452–464, doi:10.1046/j.1365-313x.2003.01819.x.
25. Liu, H.; Zhang, B.; Wu, T.; Ding, Y.; Ding, X.; Chu, Z. Copper Ion Elicits Defense Response in Arabidopsis Thaliana by Activating Salicylate- and Ethylene-Dependent Signaling Pathways. *Mol Plant* **2015**, *8*, 1550–1553, doi:10.1016/j.molp.2015.07.008.
26. Drazkiewicz, M.; Skórzyńska-Polit, E.; Krupa, Z. Copper-Induced Oxidative Stress and Antioxidant Defence in Arabidopsis Thaliana. *Biometals* **2004**, *17*, 379–387, doi:10.1023/b:biom.0000029417.18154.22.

27. Bourdais, G.; Burdiak, P.; Gauthier, A.; Nitsch, L.; Salojärvi, J.; Rayapuram, C.; Idänheimo, N.; Hunter, K.; Kimura, S.; Merilo, E.; et al. Large-Scale Phenomics Identifies Primary and Fine-Tuning Roles for CRKs in Responses Related to Oxidative Stress. *PLoS Genet* **2015**, *11*, e1005373, doi:10.1371/journal.pgen.1005373.
28. Sappl, P.G.; Carroll, A.J.; Clifton, R.; Lister, R.; Whelan, J.; Harvey Millar, A.; Singh, K.B. The Arabidopsis Glutathione Transferase Gene Family Displays Complex Stress Regulation and Co-Silencing Multiple Genes Results in Altered Metabolic Sensitivity to Oxidative Stress. *Plant J* **2009**, *58*, 53–68, doi:10.1111/j.1365-313X.2008.03761.x.
29. Anderson, S.J.; Kramer, M.C.; Gosai, S.J.; Yu, X.; Vandivier, L.E.; Nelson, A.D.L.; Anderson, Z.D.; Beilstein, M.A.; Fray, R.G.; Lyons, E.; et al. N6-Methyladenosine Inhibits Local Ribonucleolytic Cleavage to Stabilize MRNAs in Arabidopsis. *Cell Reports* **2018**, *25*, 1146-1157.e3, doi:10.1016/j.celrep.2018.10.020.
30. Wei, L.-H.; Song, P.; Wang, Y.; Lu, Z.; Tang, Q.; Yu, Q.; Xiao, Y.; Zhang, X.; Duan, H.-C.; Jia, G. The M6A Reader ECT2 Controls Trichome Morphology by Affecting MRNA Stability in Arabidopsis. *The Plant Cell* **2018**, *30*, 968–985, doi:10.1105/tpc.17.00934.
31. Zhao, X.; Li, J.; Lian, B.; Gu, H.; Li, Y.; Qi, Y. Global Identification of Arabidopsis LncRNAs Reveals the Regulation of MAF4 by a Natural Antisense RNA. *Nat Commun* **2018**, *9*, 5056, doi:10.1038/s41467-018-07500-7.
32. Li, Y.-F.; Zheng, Y.; Vemireddy, L.R.; Panda, S.K.; Jose, S.; Ranjan, A.; Panda, P.; Govindan, G.; Cui, J.; Wei, K.; et al. Comparative Transcriptome and Translatome Analysis in Contrasting Rice Genotypes Reveals Differential MRNA Translation in Salt-Tolerant Pokkali under Salt Stress. *BMC Genomics* **2018**, *19*, 935, doi:10.1186/s12864-018-5279-4.
33. FastQC 2015.
34. Bolger, A.M.; Lohse, M.; Usadel, B. Trimmomatic: A Flexible Trimmer for Illumina Sequence Data. *Bioinformatics* **2014**, *30*, 2114–2120, doi:10.1093/bioinformatics/btu170.
35. Dobin, A.; Davis, C.A.; Schlesinger, F.; Drenkow, J.; Zaleski, C.; Jha, S.; Batut, P.; Chaisson, M.; Gingeras, T.R. STAR: Ultrafast Universal RNA-Seq Aligner. *Bioinformatics* **2013**, *29*, 15–21, doi:10.1093/bioinformatics/bts635.
36. Anders, S.; Pyl, P.T.; Huber, W. HTSeq--a Python Framework to Work with High-Throughput Sequencing Data. *Bioinformatics* **2015**, *31*, 166–169, doi:10.1093/bioinformatics/btu638.
37. Love, M.I.; Huber, W.; Anders, S. Moderated Estimation of Fold Change and Dispersion for RNA-Seq Data with DESeq2. *Genome Biol* **2014**, *15*, 550, doi:10.1186/s13059-014-0550-8.
38. Zhang, Y.; Liu, T.; Meyer, C.A.; Eeckhoute, J.; Johnson, D.S.; Bernstein, B.E.; Nusbaum, C.; Myers, R.M.; Brown, M.; Li, W.; et al. Model-Based Analysis of ChIP-Seq (MACS). *Genome Biol* **2008**, *9*, R137, doi:10.1186/gb-2008-9-9-r137.
39. Anderson, S.J.; Kramer, M.C.; Gosai, S.J.; Yu, X.; Vandivier, L.E.; Nelson, A.D.L.; Anderson, Z.D.; Beilstein, M.A.; Fray, R.G.; Lyons, E.; et al. N6-Methyladenosine Inhibits Local Ribonucleolytic Cleavage to Stabilize MRNAs in Arabidopsis. *Cell Rep* **2018**, *25*, 1146-1157.e3, doi:10.1016/j.celrep.2018.10.020.
40. Li, H.; Handsaker, B.; Wysoker, A.; Fennell, T.; Ruan, J.; Homer, N.; Marth, G.; Abecasis, G.; Durbin, R.; 1000 Genome Project Data Processing Subgroup The Sequence Alignment/Map Format and SAMtools. *Bioinformatics* **2009**, *25*, 2078–2079, doi:10.1093/bioinformatics/btp352.
41. Heinz, S.; Benner, C.; Spann, N.; Bertolino, E.; Lin, Y.C.; Laslo, P.; Cheng, J.X.; Murre, C.; Singh, H.; Glass, C.K. Simple Combinations of Lineage-Determining Transcription Factors Prime Cis-Regulatory Elements Required for Macrophage and B Cell Identities. *Mol Cell* **2010**, *38*, 576–589, doi:10.1016/j.molcel.2010.05.004.

Disclaimer/Publisher's Note: The statements, opinions and data contained in all publications are solely those of the individual author(s) and contributor(s) and not of MDPI and/or the editor(s). MDPI and/or the editor(s) disclaim responsibility for any injury to people or property resulting from any ideas, methods, instructions or products referred to in the content.